Journal of Structural Geology, Vol. 9, No. 3, pp. 313 to 330, 1987
Printed in Great Britain

0191-8141/87 $03.00 + 0.00

Oblique diapirism: the Criffel granodiorite/granite zoned pluton (southwest Scotland)

G. Courrioux*

Department of Geological Sciences, University of Durham, Durham DH1 3LE, U.K.

(*Received* 14 *April* 1986; *accepted in revised form* 29 *September* 1986)

Abstract—Strain trajectories, strain gradients and quartz ⟨c⟩ fabrics have been used to propose an emplacement history of the Criffel zoned pluton. Strain has been estimated from the microdioritic xenoliths included in the outer granodiorite; textural criteria have been used to complete the pattern of strain variations throughout the pluton. Strain gradients are found to be related to the granodiorite/granite boundary zone, with highest strain towards the northeast side of the pluton, giving an asymmetric horseshoe pattern. Quartz ⟨c⟩ fabrics allow two strain histories to be distinguished within the pluton: an early coaxial flattening in the granodiorite followed by a non-coaxial deformation in the granite and the adjacent granodiorite. These features are interpreted as the result of an oblique diapiric intrusion of the inner granite into the partially emplaced and crystallized granodiorite.

INTRODUCTION

Since Ramberg's experiments on gravitational instabilities (1967, 1970), it is commonly accepted that diapirism is a major mechanism of granite emplacement. The process has been modelled by Dixon (1975) and Schwerdtner & Troeng (1978), who have shown the type of strain patterns that can be expected in and around diapirs. Brun & Pons (1980) have extended this by describing examples of strain trajectories resulting from the interference of diapirism and synchronous regional deformation. The ballooning mechanism, where deformation is the result of multiple magmatic pulses, has been described by Ramsay (1975, 1981) and Holder (1979).

Classical field evidence for diapiric intrusion includes: (a) less dense material surrounded by denser material; (b) concentric patterns of foliation within the intrusion; (c) strain increasing towards the margin of the pluton; (d) important deformation in the country rocks around the pluton; (e) conformable structures in the pluton and in the surrounding rocks; (f) horizontal extension in the crestal area of the pluton (Schwerdtner 1981). However, detailed studies of internal structures of many other granites show that plutons may exhibit more complex emplacement and deformation histories than simple diapirism. They may display combinations of diapirism, stoping, fracture controlled emplacement, or emplacement in ductile shear zones (Berger & Pitcher 1970, Blanchard 1978, Pitcher 1979, Courrioux 1982, Hutton 1982a, Gagny *et al.* 1984, Guillet *et al.* 1985). With this in mind, a detailed strain and microstructural study was undertaken on the Criffel granite in southwest Scotland.

*Present address: Laboratoire de Pétrologie Structurale et Métallogénie, UA (CNRS) 728, Université de Nancy I, 54506 Vandoeuvre lès Nancy Cédex, France.

STRUCTURAL SETTING

The Southern Uplands can be schematically described as a sequence of slices separated by strike-parallel faults. Although sediments young NW within each slice, the general younging of the sediments is SE with Wenlock turbidites occurring in the area of the Criffel pluton. The low-grade burial metamorphism and the deformation decrease and supposedly become younger towards the south (Oliver *et al.* 1984, Kemp *et al.* 1985). Some late Silurian sinistral strike–slip movement occurs along faults or within discrete shear bands (Needham 1984). These features have been ascribed to the evolution of an accretionary prism during the Ordovician and Silurian (McKerrow *et al.* 1977, Leggett *et al.* 1983). They have been alternatively interpreted as imbricate stacks combining SW-directed thrusting and sinistral shear during an oblique Silurian collision (Soper & Hutton 1984, Murphy & Hutton 1986).

In the Criffel area, the regional deformation is very low and general structures dip steeply NW. The strata are uptilted around the pluton (Phillips 1956) with strikes and outward dips parallel to the contact. Penetrative deformation in the country rocks appears to increase towards the granite and is restricted to the 1 km wide aureole (Kafafy & Tarling 1985). The characteristics of this imposed strain in the country rocks have not been studied.

THE CRIFFEL PLUTON

The pluton, early Devonian in age (397 ± 2 Ma, Halliday *et al.* 1980) intrudes the Silurian sediments of Southern Uplands. It developed a 1 km wide contact metamorphic aureole containing hornblende and diopside (Phillips 1956) in the low-grade flysch sequence. Gravity data indicate that it is about 10 km deep, i.e. less

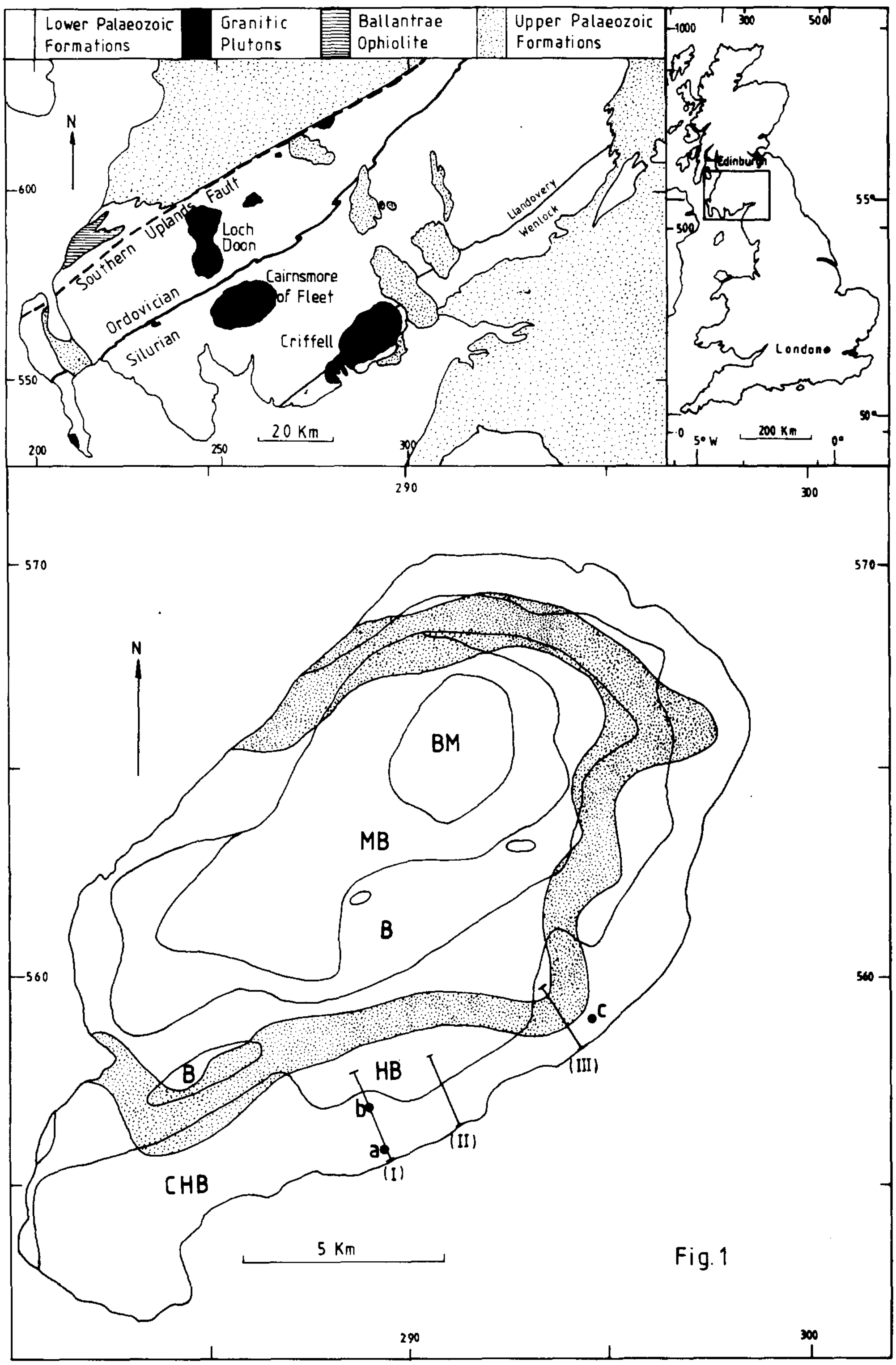

Fig. 1. Map of the petrographic facies in the Criffel plution after Stephens *et al.* (1985). CHB, clinopyroxene-hornblende-biotite granodiorite; HB, hornblende-biotite granodiorite; B, biotite granite; MB, muscovite-biotite granite; BM, biotite-muscovite granite. Dotted area, granodiorite/granite boundary zone as chemically defined by Stephens & Halliday (1980). Location of sites a, b, c of Fig. 5 and profiles I, II, III of Figs. 7–9. Kilometric grid of Great Britain.

than its areal size (23 × 11 km) (Bott & Masson-Smith 1960). The contacts dip steeply outwards to depth (Phillips 1956, Bott & Masson-Smith 1960). It is a typically zoned pluton that consists of an outer shell of granodiorite surrounding a porphyritic granite (Phillips 1956). These two main facies have been subdivided by Stephens *et al.* (1985), on the basis of mafic mineral content, into five petrographic facies (Fig. 1). Mapping the differentiation index (Thornton & Tuttle 1960) (Normative Qz + Ab + Or) has revealed an area about 2 km wide of steep geochemical gradients between the granodiorite and granite (Fig. 1). This has been interpreted as an interaction zone between two distinct magmas (Stephens & Halliday 1980). These data together with isotopic and trace element information led Halliday *et al.* (1980) and Stephens *et al.* (1985) to propose that the primary magma

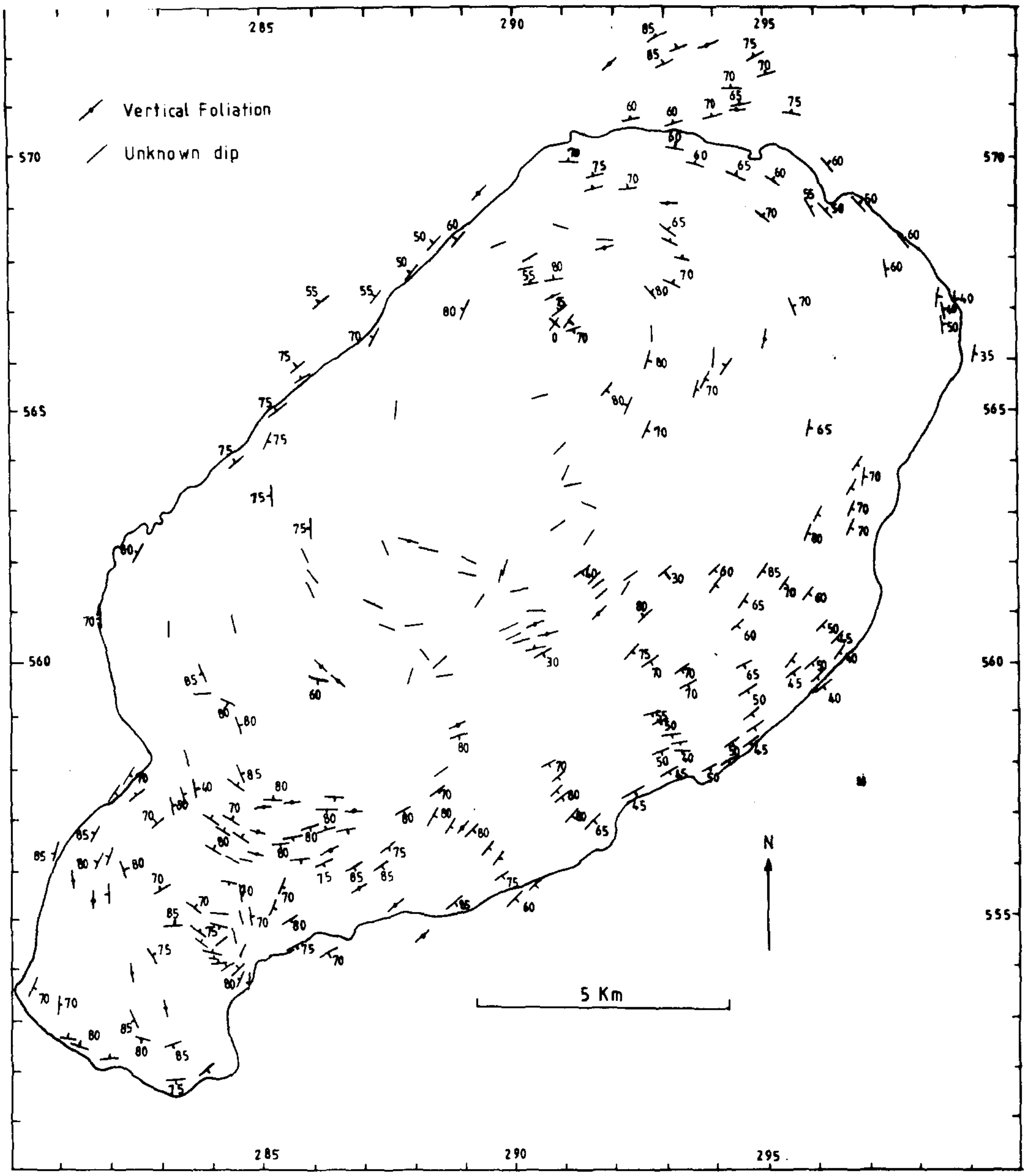

Fig. 2. Map of foliations in the Criffel pluton. Kilometric grid of Great Britain.

was of *I*-type (mantle or new oceanic crust derived), which as it rose through the crust was progressively enriched in *S*-type derived melts which accumulated as separate pulses.

The emplacement mechanism of the pluton has been the subject of debate (Bott & Smithson 1967, Coward 1981, Phillips *et al.* 1981, 1983, Holder 1983). The main argument against diapirism as a major mechanism was that the country rocks are not strongly deformed around the pluton, and therefore that stoping and convection occurred during the emplacement of the body. The aim of this study is (1) to gain precise information on the foliation trajectories, strain gradients and deformation regimes within the Criffel pluton and (2) to develop a model for the emplacement of the complex itself.

STRAIN TRAJECTORIES

The outer granodiorite shows a very well-marked anisotropy displayed by the preferred orientations of feldspar, hornblende, biotite and the elongation of quartz grains. The fabric has a strong planar character with a weak lineation defined by hornblende. The foliation and the lineation orientations are consistent with the deformation fabric implied by the shapes of microdioritic xenoliths included within this unit. The inner granite, by contrast, shows a very weak anisotropy marked by the orientation of K-feldspars and biotites. In a few cases, it has been possible to determine a lineation developed within the foliation plane. A transition zone, some 200–500 m wide, occurs between the strongly foliated granodiorite and the weakly deformed granite.

The foliation

The foliation trajectories are shown on Figs. 2 and 3. They display a general concentric pattern that broadly follows the elliptical shape of the pluton. In detail, however, it can be seen that the centres of the more internal elliptical trajectories are displaced progressively

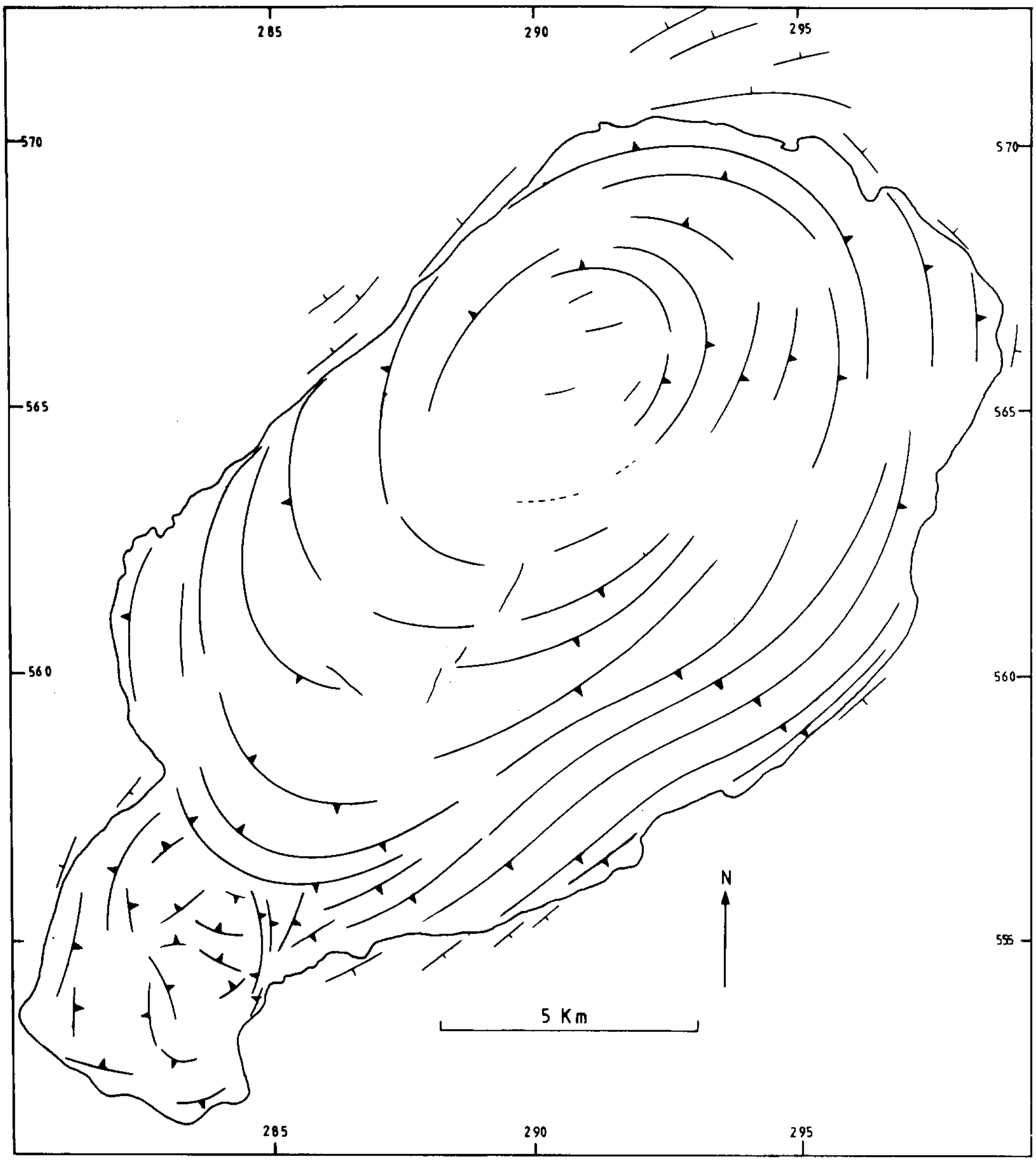

Fig. 3. Foliation trajectories in the Criffel pluton. Kilometric grid of Great Britain.

towards the northeast (Fig. 3). This follows the petrographic zonation in the pluton. There is a discordance in the geometry of the foliation trajectories in the southwest part of the pluton, where a more irregular pattern occurs. This discordance may be related to the contrasting behaviour of two parts of the intrusion. Near the contacts the foliation generally dips outwards, with the shallowest dips occurring in the southeast ($\simeq 40°$). Typically, the dips increase towards the centre, although gently-dipping and even subhorizontal foliations have been recorded in some parts of the central region.

The lineation

The lineation (Fig. 4) is, in most cases, subhorizontal except in the southern part of the pluton where it tends to be subvertical. The domain of subvertical lineations corresponds partially with the area which contains the more irregular fabric orientation. This is also the domain of low strain (see below).

STRAIN GRADIENTS

Strain has been estimated from the shape ratios of microdioritic xenoliths. Unfortunately, the inner granite does not contain such xenoliths. Therefore, this type of strain data is limited to the outcrop of the outer granodiorite in a zone about 2 km wide. Hutton (1982b) has emphasized the difficulty of using the Rf/ϕ method (Dunnet 1969, Dunnet & Siddans 1971) on deformed xenoliths in granites. Since the outcrop surfaces rarely coincide with any of the principal strain planes, an accurate 3-dimensional strain analysis is not generally possible. However, it is possible to find planes perpendicular to the foliation and inclined at various angles θ with respect to the horizontal line contained in the foliation. Variations of axial ratios (L = long ellipse axis, l = short ellipse axis) against the angle θ should reflect the ellipsoid shape (K values) and should allow an assessment of the X/Y and X/Z ratios of the strain ellipsoid (Fig. 5). The variability of axial ratios ($\log_{10} L/l$)

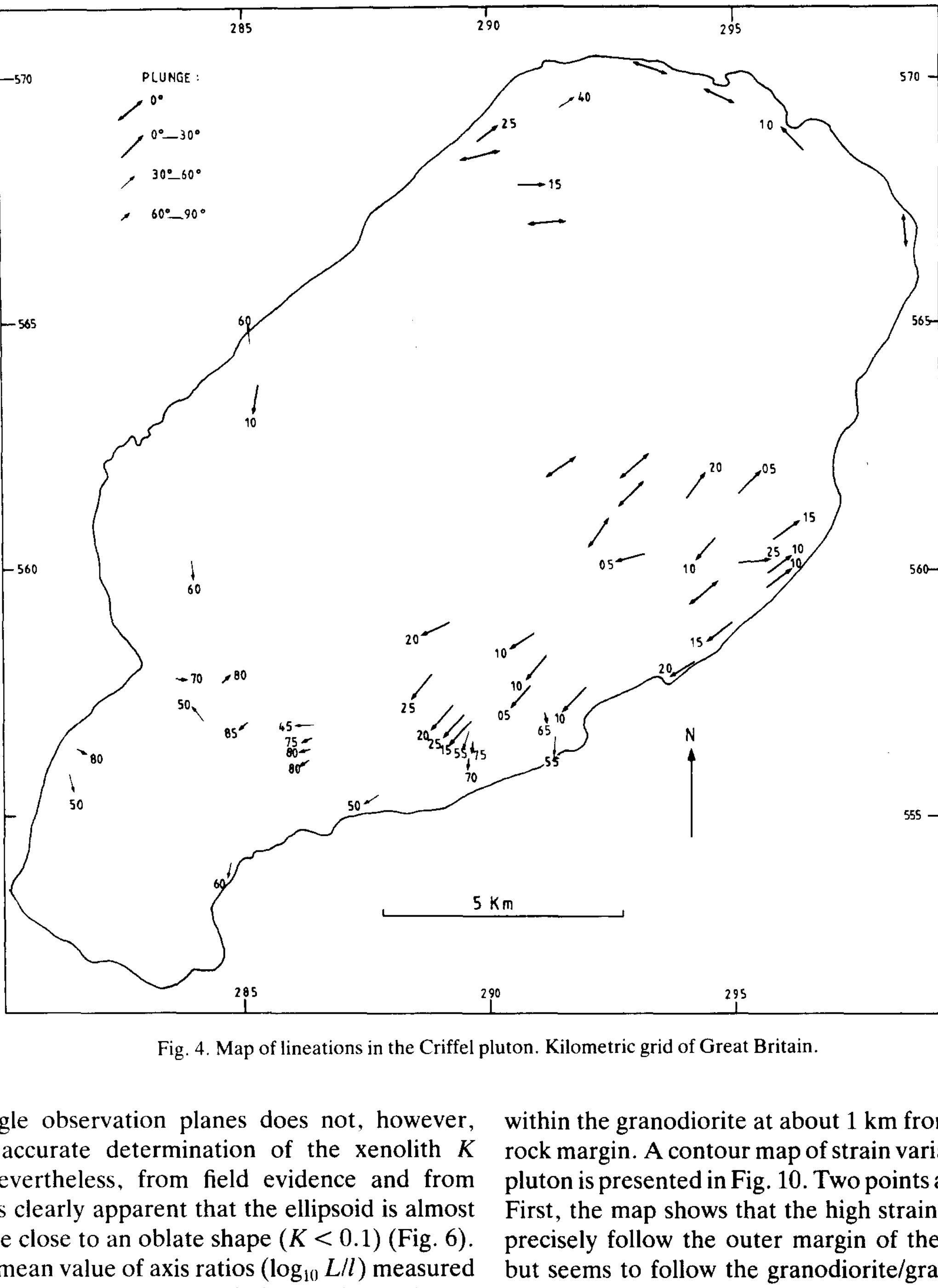

Fig. 4. Map of lineations in the Criffel pluton. Kilometric grid of Great Britain.

within single observation planes does not, however, allow an accurate determination of the xenolith K values. Nevertheless, from field evidence and from Fig. 5, it is clearly apparent that the ellipsoid is almost everywhere close to an oblate shape ($K < 0.1$) (Fig. 6). Thus, the mean value of axis ratios ($\log_{10} L/l$) measured in any orthogonal plane to the foliation can be used as an estimate of strain intensity. Though this value may be an overestimate of strain, it is reasonable to assume that this gives a good picture of the strain gradients within the pluton (Ramsay 1975, Holder 1979, Lagarde & Choukroune 1982). Furthermore, subspherical xenoliths have been observed in the less deformed parts of the pluton (L/l = 1.1, L/l = 1.2), which suggests that the errors involved in strain determination are fairly small.

Strain gradients

Three profiles, located on the southeast side of the pluton, are shown in Figs. 7–9. The first and second profiles (Figs. 7 and 8) show clearly that strain increases from the outer margin towards the interior of the pluton. The third profile (Fig. 9) displays a strain culmination within the granodiorite at about 1 km from the country-rock margin. A contour map of strain variations over the pluton is presented in Fig. 10. Two points arise from this. First, the map shows that the high strain area does not precisely follow the outer margin of the granodiorite, but seems to follow the granodiorite/granite boundary zone as defined chemically by Stephens & Halliday (1980) (Fig. 11). Second, the highest strain does not occur everywhere around the pluton, but is concentrated in the north, east and southeast sides, giving an asymmetric pattern to the strain distribution (horseshoe pattern).

This strain field has some similarity with the strain field calculated for the expansion of a cylindrical igneous contact (Morgan 1980). The necessary stretching of a surface element is greater for a smaller initial radius; but in the case of the Criffel pluton, the deformation has taken place within the pluton itself.

TEXTURAL VARIATIONS

To augment the xenolith strain data, a textural study of the deformation was undertaken throughout the plu-

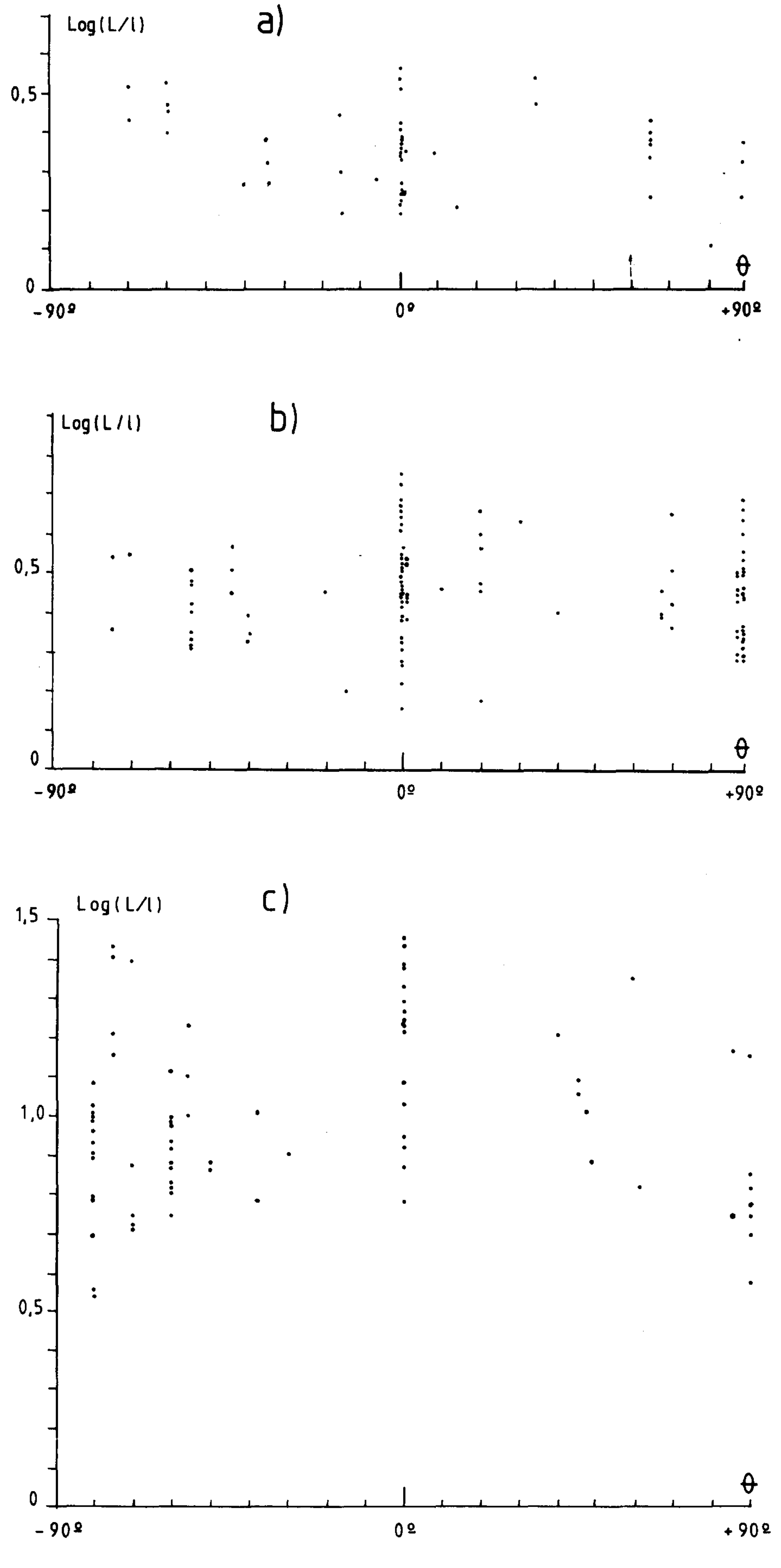

Fig. 5. Determination of K-values from xenolith axial ratios (L/l, L = long xenolith axis, l = short xenolith axis) measured in planes perpendicular to the foliation and inclined at various angles (θ) with respect to the horizontal line contained in the foliation plane. (a) $X/Z = Y/Z = 2.4$, $K < 0.1$; (b) $X/Z = 3.2$, $Y/Z = 2.8$, $K = 0.07$; (c) $X/Z = 15$, $Y/Z = 8.3$, $K = 0.11$. X = ellipsoid long axis, Y = ellipsoid intermediate axis, Z = ellipsoid short axis; $K = (X/Y - 1)/(Y/Z - 1)$.

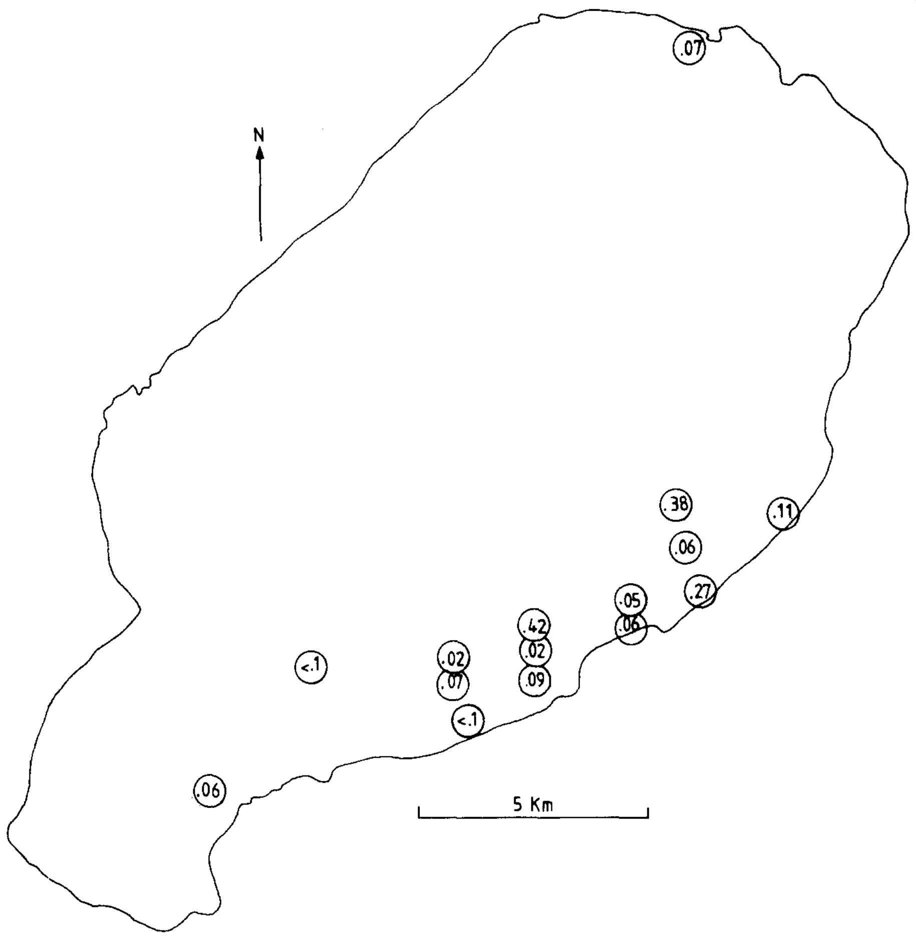

Fig. 6. *K*-values of xenolith shape-ratios in the Criffel pluton.

ton. This was based on a 1 km square grid sampling previously used by Stephens & Halliday (1980) for their geochemical study. A qualitative assessment of the amount of plastic deformation in a granite can be made based on the following criteria (Figs. 12–14). At low strains quartz is typically in the form of coarse grains with rare undulatory extinction. With increasing strain undulatory extinction becomes common and numerous sub-grain boundaries are observed. At the beginning of dynamic recrystallization the first small new grains occur; at higher strains, with advanced dynamic recrystallization, new grains are very common (Fig. 12). Rare kink bands are observed in biotite at low strains (Fig. 13), whereas with increasing deformation, important twisting and kinking occur; at higher strains biotite is recrystallized in the well-defined foliation planes, and shear bands are locally developed. A lack of grain-boundary recrystallization in feldspar is indicative of low plastic strain, whereas this feature becomes important at high plastic strains (Fig. 14).

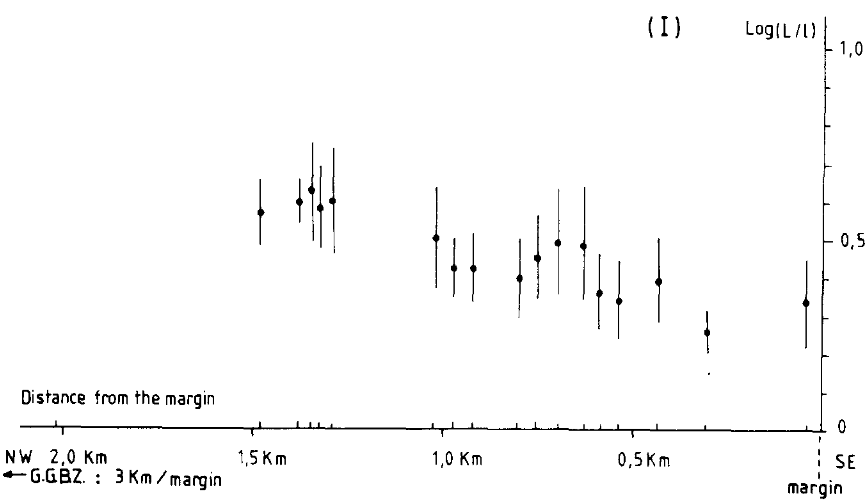

Fig. 7. Logarithmic mean values of xenolith axial ratios (*L*/*l*) measured in any plane perpendicular to the foliation plane (see profile I location in Fig. 1). Bars represent the standard deviation. G.G.B.Z.: granodiorite/granite boundary zone.

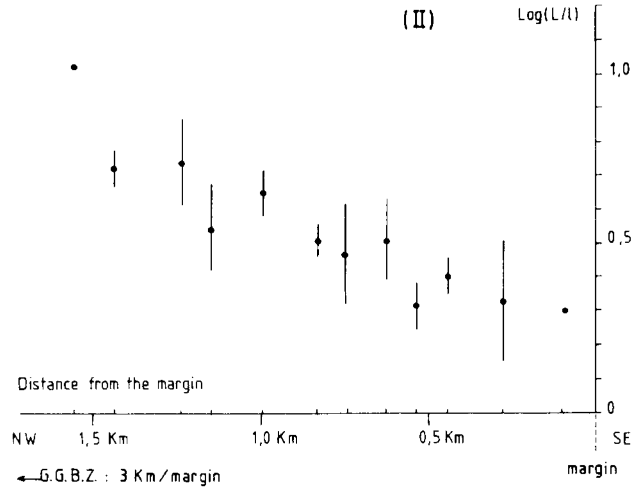

Fig. 8. Logarithmic mean values of xenolith axial ratios (*L/l*) measured in any plane perpendicular to the foliation plane (see profile II location in Fig. 1). Bars represent the standard deviation. G.G.B.Z.: granodiorite/granite boundary zone.

Textural variations (Fig. 15) show a good general agreement with the strain pattern. The area with shear-band development coincides with the highest values of strain (log $L/l > 1$). The zone with important dynamic recrystallization of quartz and with the biotite largely recrystallized in the foliation planes coincides with the high strain area (log $L/l > 0.6$). In the same way, this zone does not precisely follow the outer margin of the granodiorite, but rather the granodiorite/granite boundary zone, and it displays a similar asymmetric horseshoe pattern to the xenolith strain data. This close correlation supports the use of microdioritic xenoliths as strain markers. The maps also allow the description of deformation gradients in the inner granite where xenoliths are absent. All three textural maps show that deformation increases from southwest to northeast: a low deformation area is particularly well defined in the southwestern part of the granite. Quartz displays a regular progradation of plastic deformation from southwest to northeast parallel to the long axis of the pluton. The low deformation area does not coincide with the structural centre (approximate centre of strain trajectories) nor does it coincide with the geochemical centre (most silicic zone).

QUARTZ ⟨c⟩ FABRICS

The textural and strain features described above favour a composite intrusion. Strain patterns are most likely to be linked with the intrusion of the inner granite into the granodiorite than to the intrusion of the granodiorite itself. This hypothesis can be further tested using quartz ⟨**c**⟩ fabrics to determine whether they show a composite history.

Results

The data can be divided into two groups (Fig. 16).

(1) Samples in the vicinity of the granodiorite margin (1, 7, 8, 33, 37, 43) are weakly deformed (except 33 which is more deformed) and show a very weakly defined lineation. They tend to display quartz ⟨**c**⟩ axis concentrations in small circles around the shortening axis *Z* with an opening angle of about 40°. No significant asymmetries are observed within these diagrams. Sample 33 shows a typical complete type 1 symmetric crossed girdle.

(2) Samples of the more deformed granodiorite in the strain culmination area (6, 11, 25, 27, 32, 48), in the granodiorite/granite boundary zone (35, 40) and in the slightly deformed granite (15, 41, 42) show quartz ⟨**c**⟩ diagrams with essentially single girdles centred around *Y*. Weak concentrations in small circles around *Z* appear in some cases but are not the main characteristic of the fabrics in these samples. The girdles display a clear asymmetry with respect to lineation and foliation. The

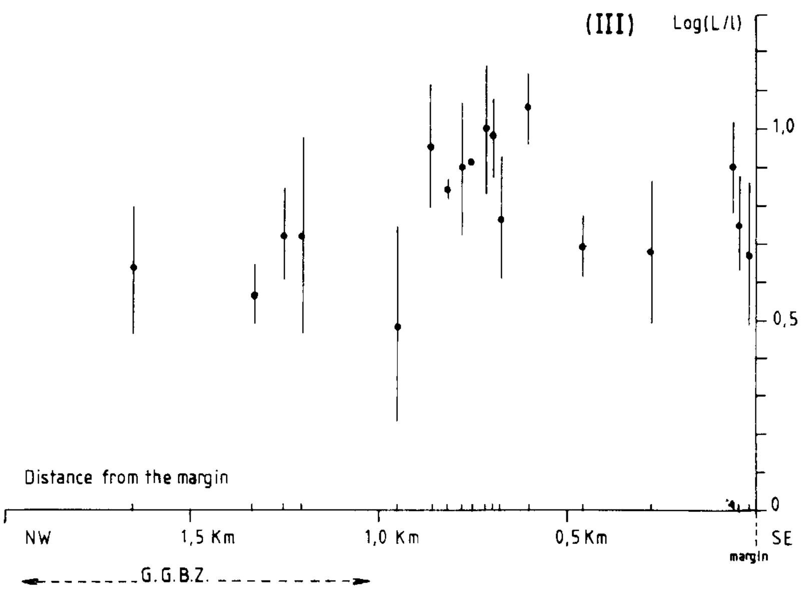

Fig. 9. Logarithmic mean values of xenolith axial ratios (*L/l*) measured in any plane perpendicular to the foliation plane (see profile III location in Fig. 1). Bars represent the standard deviation. G.G.B.Z.: granodiorite/granite boundary zone.

Fig. 10. Contour map of the mean logarithmic xenolith axial ratios over the Criffel pluton. Contours have been machine drawn at the University of St Andrews using an interpolation method based on inverse distance weighting on the four nearest points (Sampson 1975). Measurement sites are indicated by small filled circles.

profile across the strain culmination from the weakly deformed granite to the more highly deformed granodiorite shows that these concentrations develop in an asymmetric manner. In sample 15 for example, the most weakly deformed, first concentrations appear around Y and already have asymmetries consistent with other more deformed samples.

Discussion

On the basis of experimental deformation (Tullis *et al.* 1973) and numerical modelling (Lister & Hobbs 1980), the type of concentration in group (1) is generally interpreted as resulting from a coaxial flattening deformation. This is in agreement with the type of ellipsoid deducted from the xenolith shapes. The type of concentration in group (2) is interpreted as resulting from a non-coaxial deformation. Since no significantly different patterns occur between the different units of this group, it is likely that these fabrics developed in the granite, in the granite/granodiorite boundary zone, and in the granodiorite as a result of the same non-coaxial deformation event. From theoretical simulations (Etchecopar 1977, Lister & Williams 1979, Lister & Hobbs 1980) and from natural examples (Bouchez 1977, Bouchez & Pecher 1976, 1981, Gapais 1979, Berthé *et al.* 1980, Courrioux 1982, Law *et al.* 1984) it is now well demonstrated that asymmetric single girdles provide a reliable shear sense criterion (see Bouchez *et al.* 1983, Simpson & Schmid 1983, for a discussion of the problem). Thus the diagrams from the northern part of the pluton are consistent with sinistral shear, whereas the diagrams from the southern part are consistent with dextral shear along the high strain area. In addition, though only sample 25 shows microscopic evidence of non-coaxial dextral deformation, dextral shear bands have been observed in the latter area. Samples 6 and 11, which show an inclined lineation towards the south (respectively 45° and 25°) are at the transition between vertical and horizontal lineation domains and display a clear non-coaxial pattern that indicates the development of dextral shear consistent with the lineation direction. This suggests that the change in lineation attitude from subvertical to subhorizontal is associated with the development of a non-coaxial regime.

Several hypotheses that relate these two fabric types can be discussed.

(1) The symmetric patterns could be erroneously interpreted as coaxial because of the parallelism between the fabrics and the shear direction in a progressive non-coaxial deformation. Many natural examples show that even in highly sheared mylonites, there is never a strict parallelism between the girdle and the normal to the shear direction. Indeed, in the present study symmetric patterns occur in weakly deformed granodiorites, whereas non-coaxial patterns occur in more deformed granodiorite. Thus, this hypothesis is very unlikely.

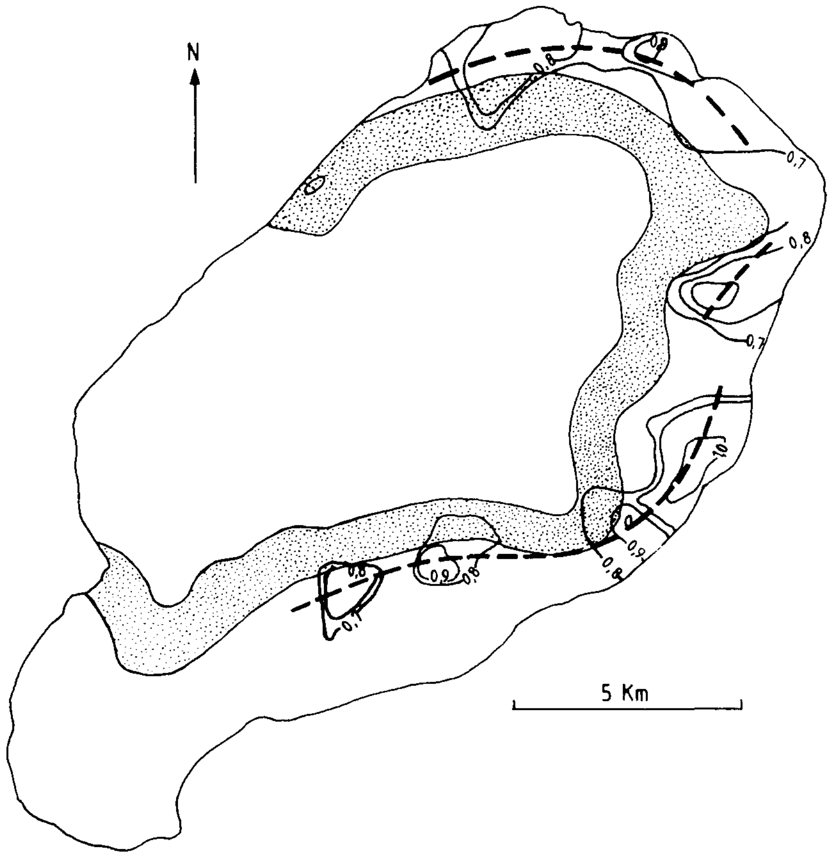

Fig. 11. Strain culmination area deduced from Fig. 10, and the granodiorite/granite boundary zone (stippled area) as defined chemically by Stephens & Halliday (1980).

(2) It could be argued that the observed variations in fabric type are linked to changes in the operative slip systems of quartz during deformation. Although quartz ⟨c⟩ diagrams alone do not allow an accurate determination of slip systems (see Schmid *et al.* 1981), the types of fabric observed here can be generally interpreted in terms of a combination between rhombohedral and prismatic slip. Both types of diagram display submaxima symmetrically disposed around *Y*, suggesting that rhombohedral slip is equally active. Numerical simulations (Lister & Hobbs 1980) tend to show that the same combination of prismatic and rhombohedral slip can account for the observed fabric variations if different strain paths are assumed. Further, even if the operative slip systems change during deformation, there is no reason why new concentrations should suddenly occur symmetrically. It is therefore unlikely that a change in operative slip systems is the main factor controlling the pattern variations, and they are more likely linked to different deformation regimes. Thus, a single non-coaxial progressive deformation event cannot account for the fabric variations observed in this study.

(3) There is an overprint of non-coaxial fabrics by a later flattening stage of the pluton. Lister & Williams (1979) have shown that a late coaxial deformation superposed on non-coaxial fabrics results in a symmetric pattern in terms of the skeleton outline but in an asymmetric pattern in terms of a density distribution. However in the present examples no significant asymmetries of density distributions have been observed.

(4) There is an overprint of early coaxial fabrics by a non-coaxial deformation developing in the granite. This remains the most likely hypothesis: any strain increase in the pluton leads to a non-coaxial pattern [this can be used also against hypothesis (3)]. Actually, the two deformations are not necessarily superposed since they may not necessarily occur in the same areas. However, clear changes are observed in closely spaced samples and it is reasonable to assume that these samples have the early stage of deformation in common.

Therefore, it is possible to conclude that a coaxial deformation occurred in the granodiorite and was then followed by a non-coaxial deformation developing within the granite and the adjacent granodiorite. In some areas, the early stage of deformation is preserved.

DISCUSSION

Emplacement of the inner granite

The features presented above can be interpreted as the result of a diapiric evolution of the inner granite. The basic model suggested here is that the granite was emplaced forcefully into the already emplaced and almost crystallized granodiorite. The ballooning produced an important deformation associated with a horizontal stretching at the edge of the granite itself and in the granodiorite. It is suggested that the intrusion direction was inclined upwards towards the northeast. This has

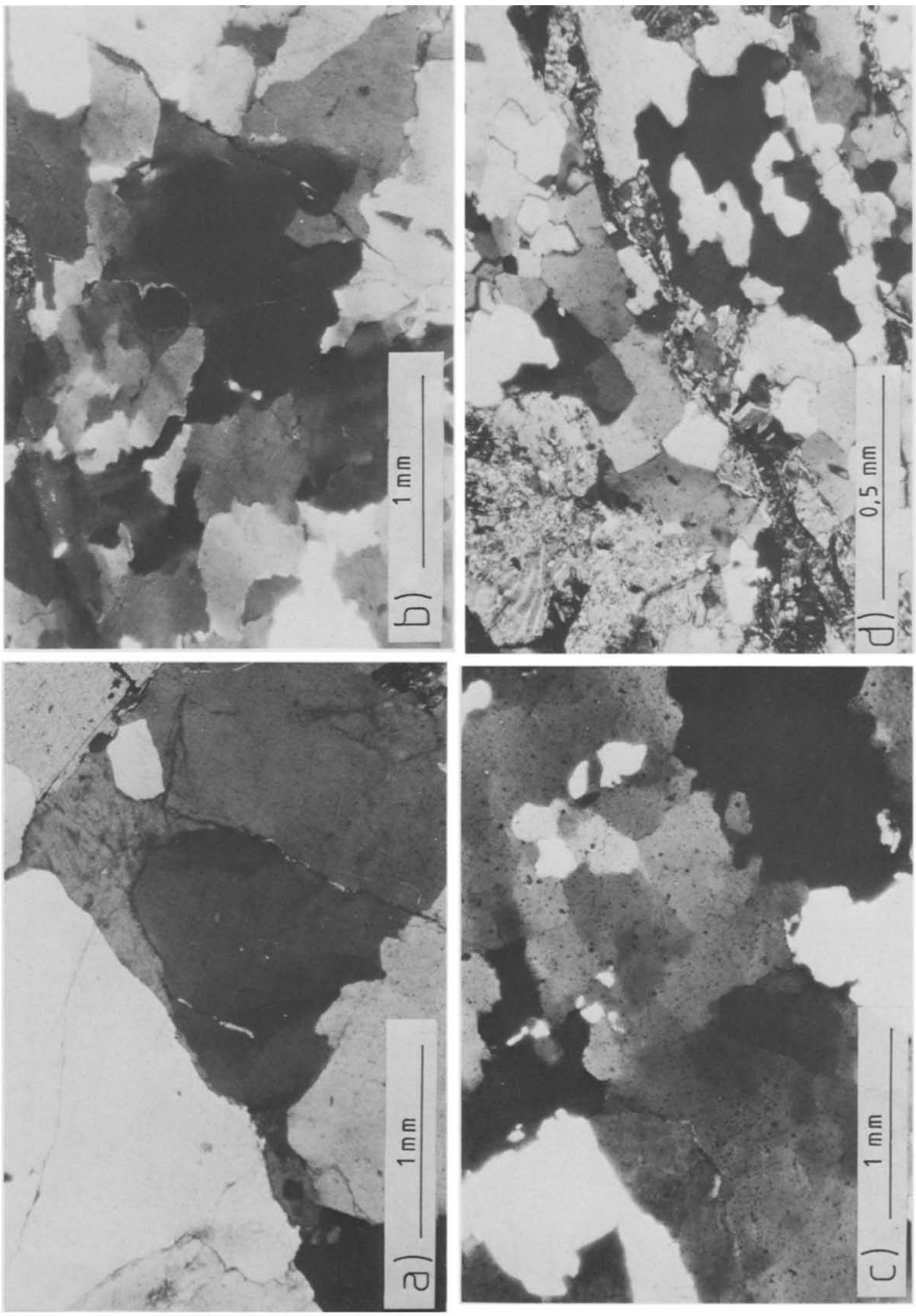

Fig. 12. Textural criteria chosen in quartz for Fig. 15. (a) Coarse grains with rare undulatory extinction. (b) Abundant *undulatory extinction and sub-grain boundaries*. (c) *Occurrence of first new grains*. (d) *Important dynamic recrystallization, numerous new grains.*

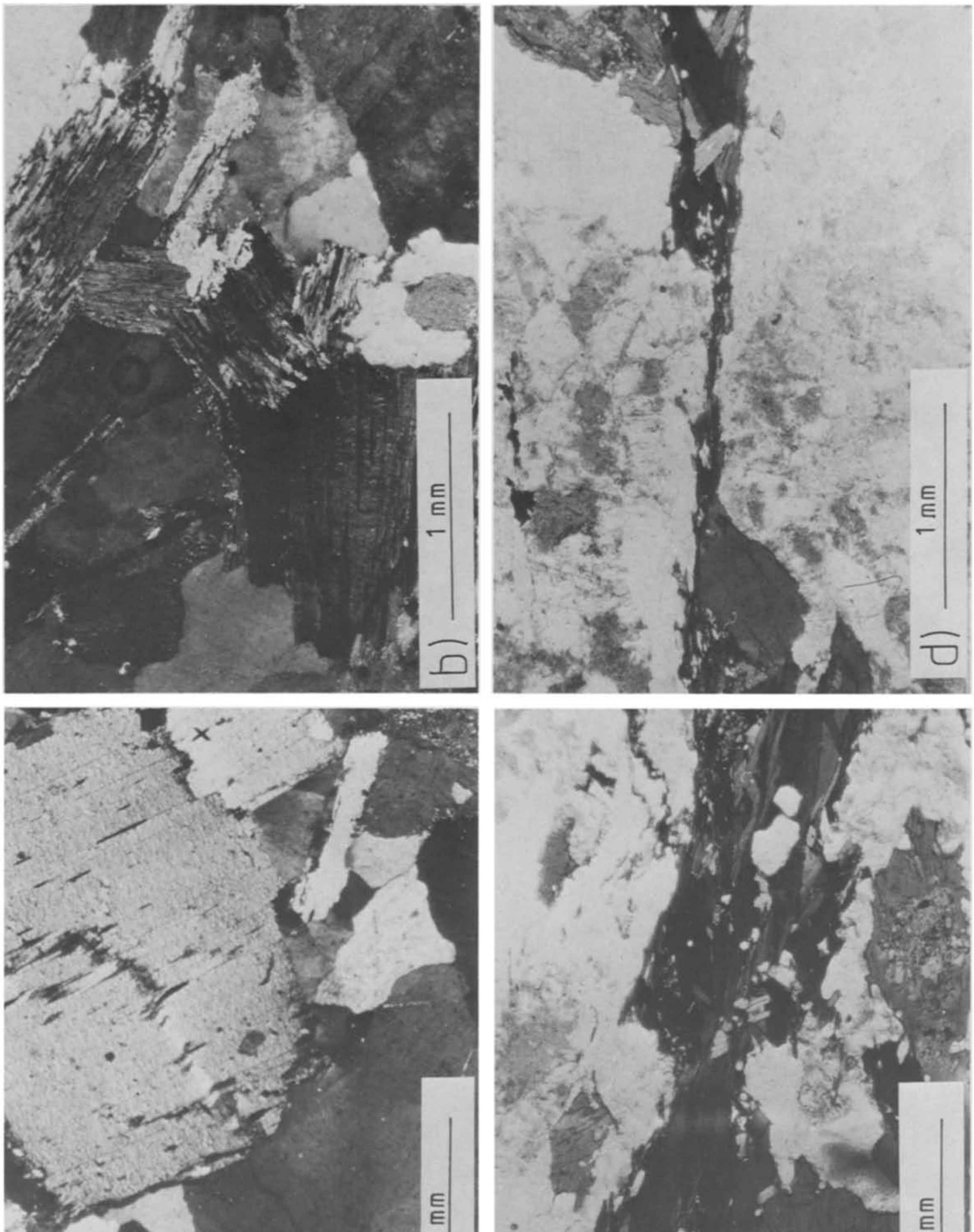

Fig. 13. Textural criteria chosen in biotite for Fig. 15. (a) Rare kink-bands. (b) Important twisting and kinking with the beginning of recrystallization. (c) Important recrystallization within the well-defined foliation plane. (d) Dextral shear band in southeast of the pluton.

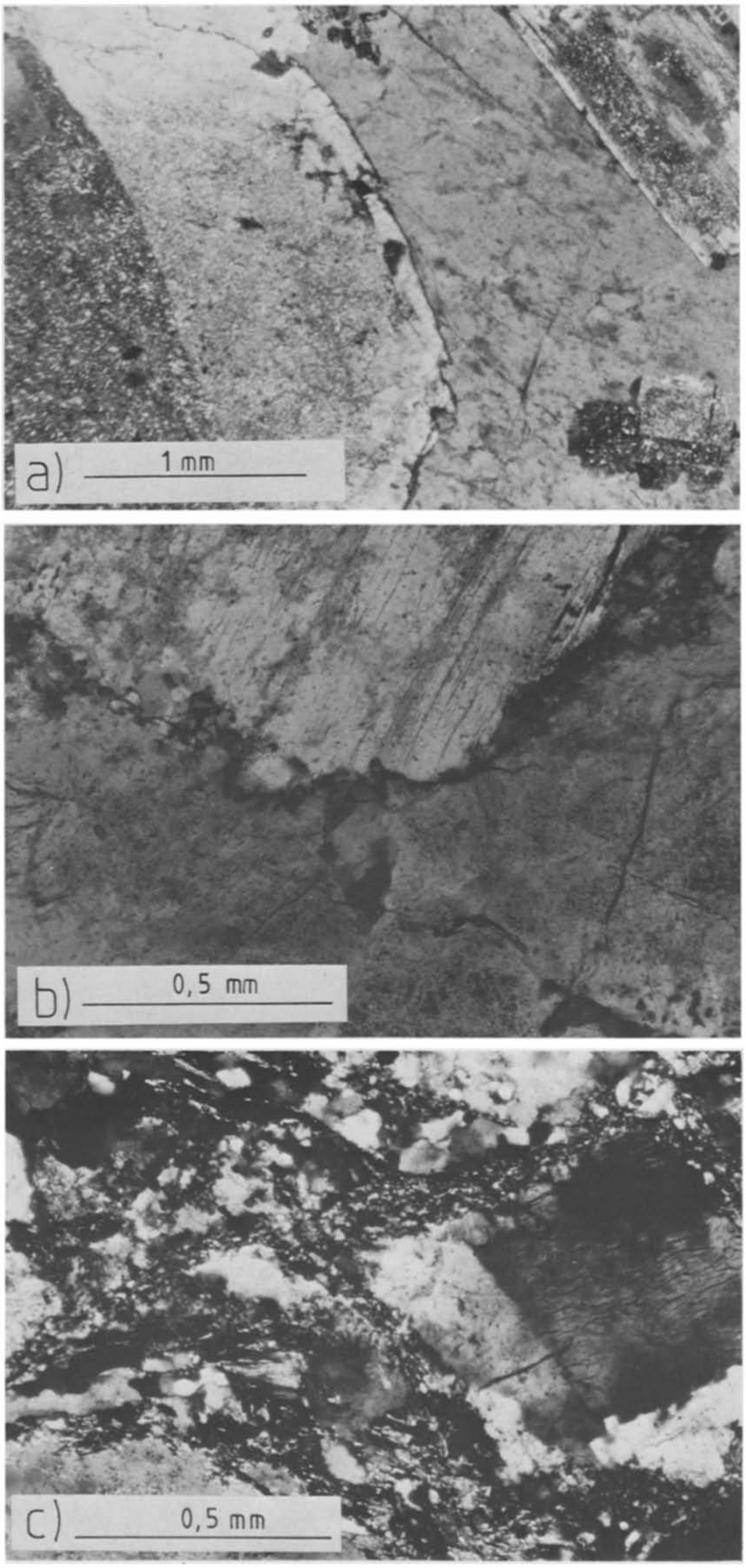

Fig. 14. Textural criteria chosen in feldspar for Fig. 15. (a) No grain-boundary recrystallization. (b) Weak grain-boundary recrystallization. (c) Important grain-boundary recrystallization.

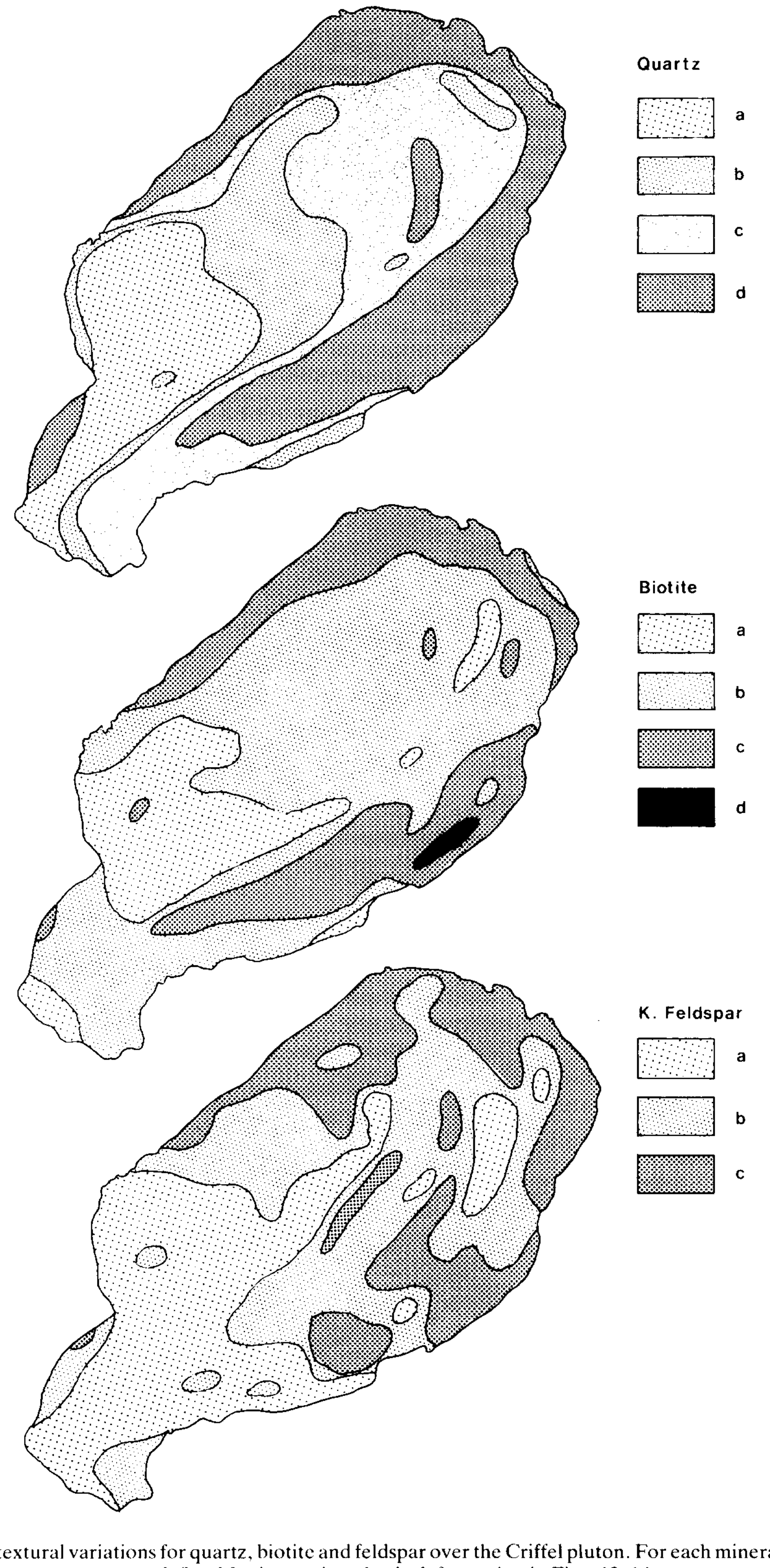

Fig. 15. Maps of textural variations for quartz, biotite and feldspar over the Criffel pluton. For each mineral, textural criteria are defined for increasing plastic deformation in Figs. 12–14.

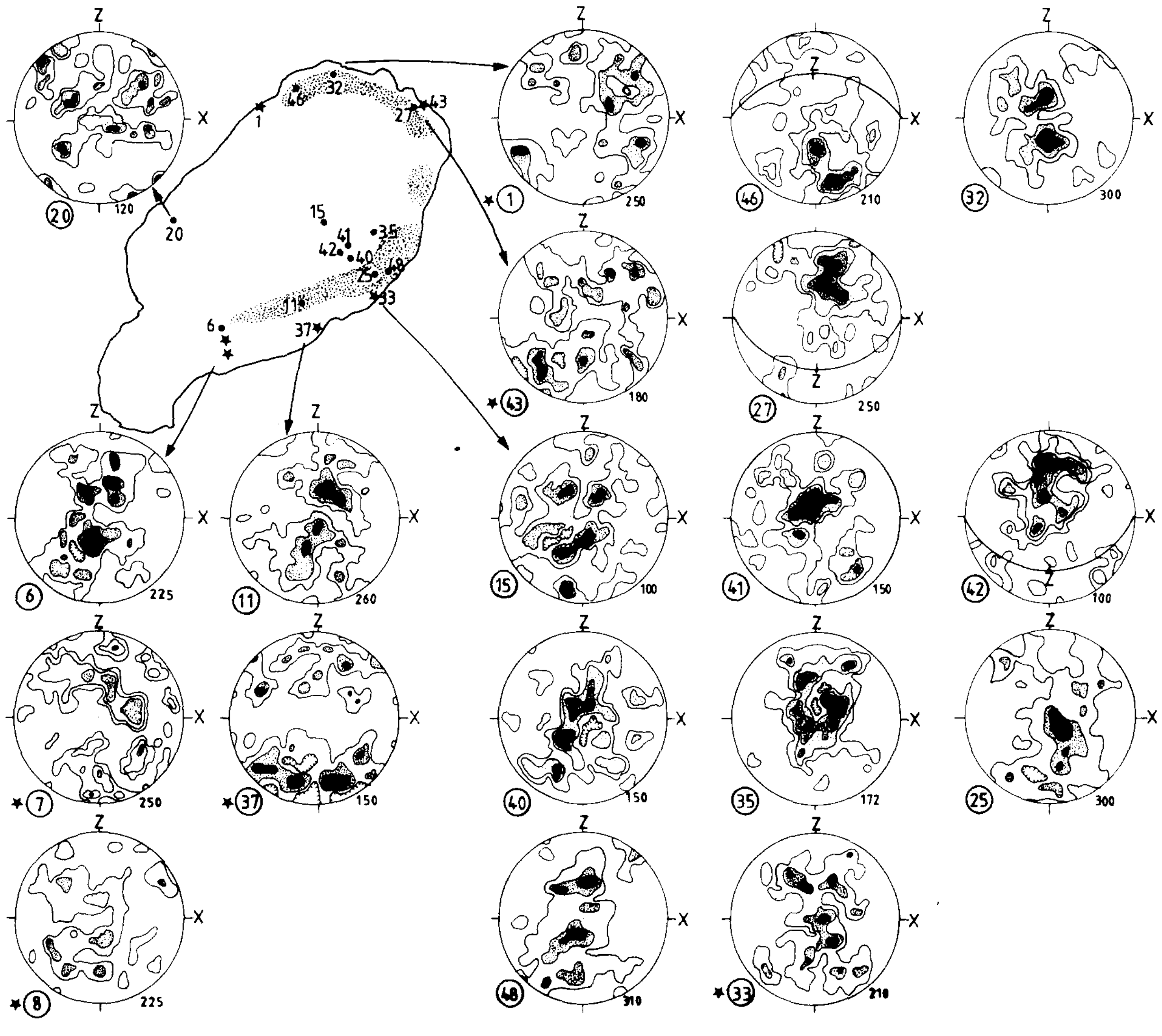

Fig. 16. Quartz ⟨c⟩ diagrams over the Criffel pluton. Lower hemisphere equal area projections. Contours are 1, 2, 3, . . . x uniform distribution. Diagrams are oriented with respect to the lineation (X) and the pole to foliation (Z). For all diagrams, the foliation is steeply inclined outwards from the pluton and parallel to the contact. In diagrams 8, 7, 6, and 11, the lineations dip to the south at angles of 80°, 80°, 45° and 25°, respectively. For all other diagrams, the lineation is subhorizontal. Diagram numbers are indicated at bottom left of each diagram. Number of ⟨c⟩ axis measurements are indicated at bottom right. Diagrams labelled with a star are referred to as symmetric patterns in the text.

resulted in the observed horse-shoe pattern of strain variations in the granodiorite and in the progradation of plastic deformation towards the north in the granite. This oblique intrusion leaves the southern part partially undeformed and accounts for lineation attitude variations (steeply inclined to the south in the low deformation area and becoming horizontal with increasing deformation). Reverse shear senses in the northern and southern part of the pluton can be interpreted as caused by lateral movement of the expanding body preferentially towards the northeast, resulting in shear deformation in the granite and the adjacent granodiorite at the two margins parallel to transport direction.

Discussion on granodiorite/granite emplacement

It seems quite clear that the Criffel pluton is at least a two-component intrusion. Although the emplacement of the inner granite can be understood in terms of oblique diapirism and ballooning, the emplacement of the granodiorite is more difficult to understand, since it has been deformed by the later intrusion. However, quartz ⟨c⟩ fabrics have recorded an earlier coaxial flattening event in some places of the granodiorite and indicate that the ballooning mechanism was also probably involved in the earlier phase of pluton emplacement.

Although a behaviour contrast exists between granite and granodiorite at the time of granite emplacement, lineations are found to be concordant in both components, suggesting that the two intrusions may have followed closely in space and time. The heat of the first intrusion may have created partial melting in the crust (Hallyday 1983, Stephens *et al.* 1985); and the melts may have coalesced into a single granitic mass, less dense than the already partially crystallized granodiorite. Consequently, the granite could have risen more rapidly and reintruded the granodiorite at a higher level. The granodiorite may have been flattened by its own intrusion, or it may have been flattened by the granitic

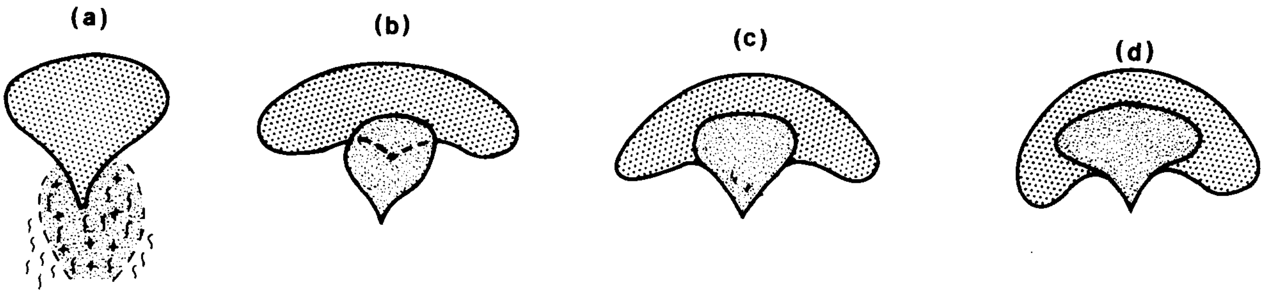

Fig. 17. Possible relations between granodiorite and granite emplacement. (a) Granodiorite emplacement and partial melting of the underlying crust. (b) Flattening of the granodiorite. (c) Bending of the denser granodiorite around the rising granite diapir. (d) Final shape after ballooning of the granite.

intrusion and then was subsequently bent around the granite as it became too dense to go on rising (Fig. 17).

Pluton geometry

The final geometry implied by the evolution described above is represented in the asymmetric case in Fig. 18. It is compatible with the dip variations of the foliation in the eastern part of the pluton (i.e. increase in fabric steepness from the margin towards the core). However this is not particularly compatible with the vertical lineation and very steep foliations in the southwest part of the pluton.

The second possibility is that the granite did not deform the tail of the granodiorite but was emplaced to one side of it, as shown in Fig. 19. In this case, the southern part of the pluton would represent the root of the granodiorite, which itself therefore would have been emplaced obliquely. This model has the advantage of fitting the foliation and lineation variations and the strain gradients throughout all of the pluton.

Both geometries are compatible with the gravity interpretation of the pluton shape at depth (Bott & Masson-Smith 1960). A single diapir with contacts dipping outwards to 10 km would imply the existence of a huge batholith if a classical diapiric shape with lower inward dipping contacts was assumed. The mushroom shape suggested here fits the gravity data and leads to smaller space accommodation problems. Indeed, high penetrative deformation in the country rocks is restricted to the zone of contact metamorphism (1 km wide), and deformation can be accommodated within larger distances. Furthermore, the ballooning granite deformation is partially accommodated within the granodiorite.

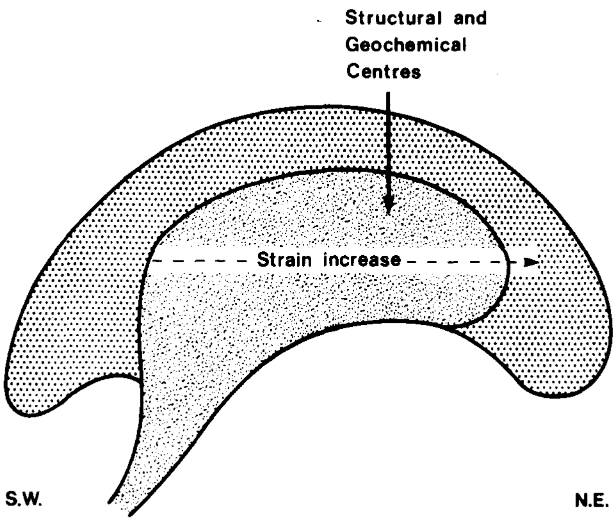

Fig. 18. Geometric relations between the granodiorite and the granite in the case of an oblique intrusion of the inner granite into the granodiorite where the former deforms the tail of the granodiorite as in Fig. 17.

Possible reasons for an oblique intrusion

A subsequent northeastward tilting after granite emplacement should be apparent in the disposition of the Silurian rocks. Similarly it might have resulted in obvious important post-Devonian deformation and faulting. There is no evidence for either of these effects and the tilting hypothesis is therefore very unlikely. This leaves two other possibilities. Firstly that the pluton was affected by an inclined regional strain field, produced for example by a combination of SE-directed overthrusting and sinistral shear affecting the entire region at this time. Secondly, following Talbot's experiments (Talbot 1977), asymmetry could have been produced by an inclined magmatic source layer. Neither of these possibilities is entirely satisfactory. An inclined sinistral strain field should have sheared the granite in a dominantly sinistral sense, which it does not. An inclined layer is likely to be a fairly large scale regional feature, and yet none of the other (synchronous) plutons of the Southern Uplands appear to show the style of asymmetry of Criffel. However, smaller scale lateral variations in source layer density and/or viscosity (Talbot 1977) in the Criffel pluton is a remaining possibility.

CONCLUSIONS

Conclusions can be summarized as follows:

(1) The distribution of strain gradients shows that most of the deformation within the granodiorite is related to the diapiric emplacement of the inner granite.

(2) From the strain trajectories, strain distribution and textural variations (horseshoe pattern), it is inferred that ballooning has been asymmetric resulting from an intrusion direction inclined up towards the northeast.

(3) Quartz ⟨c⟩ fabrics suggest two distinct deformation

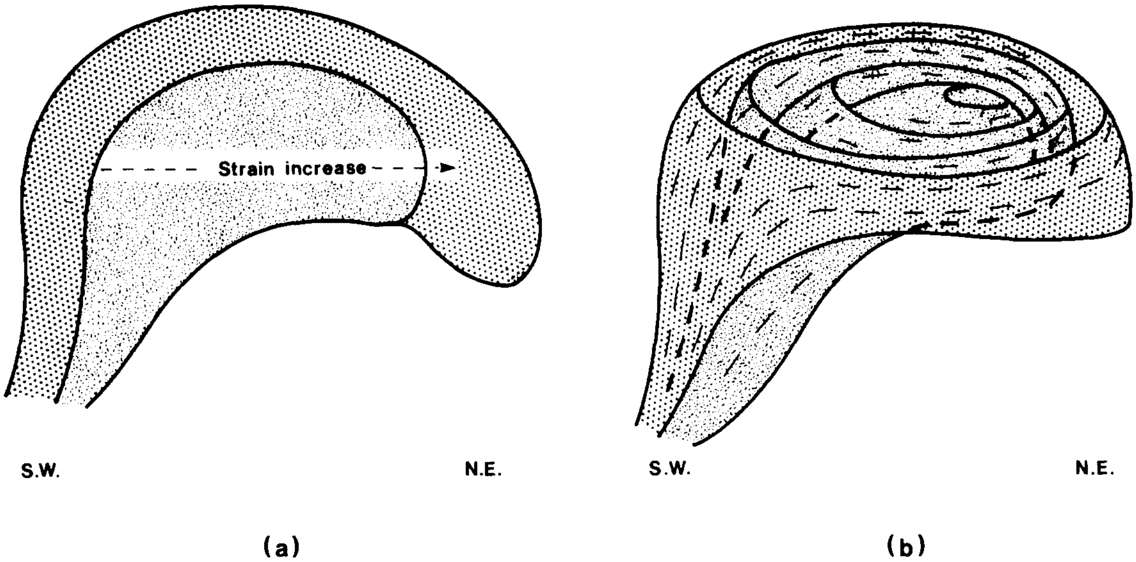

Fig. 19. (a) Geometric relations between granodiorite and granite where the granite rises obliquely on the side of the granodioritic tail. (b) Foliation and lineation trajectories.

regimes, that are interpreted as evidence of at least a two-stage deformation during the intrusion history. An early flattening coaxial deformation is displayed in the granodiorite and is marginally overprinted by a non-coaxial deformation that consistently affects the granite and the adjacent granodiorite.

(4) The senses of shear deduced from quartz-fabric asymmetries are compatible with the lateral expansion of the granite implied by this model.

(5) Two models of relation between granodiorite and granite emplacement are discussed. In the first model, the granite intrusion deforms the tail of the granodiorite and flattens it. In the second model the granite rises on the side of the tail leaving it undeformed, both components rise obliquely and then laterally expand as suggested by the lineation trajectories.

(6) Though strain trajectories and strain gradients favour the second hypothesis, the data presented here do not allow an accurate understanding of the early stage of the granodiorite emplacement. Only the oblique intrusion of the inner granite and its effects on the already partially emplaced and crystallized granodiorite are well demonstrated.

(7) The reason for oblique diapirism in this area of the Southern Uplands is not clear.

(8) More strain data would be necessary in the weakly deformed granodiorite to characterize the initial strain gradients, and in the country rocks to see whether the two intrusion stages have distinguishable effects.

Acknowledgements—I would like to express my thanks to Donny Hutton for having provided the opportunity of working on the Criffel Pluton and for his constant help during the preparation of the manuscript; I would like also to thank Edryd Stephens who introduced me to the area, provided the thin sections of the textural study and for the strain contouring at the University of St Andrews. I acknowledge Jean Pierre Brun and John Dixon whose helpful reviews improved the paper, and John Dewey for his comments on the manuscript. This study was achieved while the author was holding a one year post-doctoral research fellowship from The British Council at the University of Durham.

REFERENCES

Berger, A. R. & Pitcher, W. S. 1970. Structures in granitic rocks: a commentary and a critique on granite tectonics. *Proc. Geol. Ass.* **81**, 441–461.

Berthé, D., Choukroune, P. & Gapais, D. 1979. Orientations préférentielles du quartz et orthogneissification progressive en régime cisaillant: l'exemple du cisaillement sud armoricain. *Bull. Minéral.* **102**, 265–272.

Blanchard, J. Ph. 1978. Dynamique magmatique du granite porphyroide des Ballons (Vosges meridionales). "Fluidalités planaires imbriquées" et "couloirs magmatiques". Phénomène de percolation. *Bull. Soc. géol. Fr.*, 7 *Ser.*, **XX**, 157–162.

Bott, M. H. P. & Masson-Smith, D. 1960. A gravity survey of the Criffel granodiorite and the New Red Sandstone deposits near Dumfries. *Proc. Yorks. geol. Soc.* **32**, 317–332.

Bott, M. H. P. & Smithson, S. B. 1967. Gravity investigations of subsurface shape and mass distributions of granite batholiths. *Bull. geol. Soc. Am.* **78**, 859–878.

Bouchez, J. L. 1977. Plastic deformation of quartzites at low temperature in an area of natural strain gradients. *Tectonophysics* **39**, 25–50.

Bouchez, J. L., Lister, G. S. & Nicolas, A. 1983. Fabric asymmetry and shear sense in movement zones. *Geol. Rdsch.* **72**, 401–419.

Bouchez, J. L. & Pecher, A. 1976. Plasticité du quartz et sens de cisaillement dans les quartzites du Grand Chevauchement Central Himalayen. *Bull. Soc. géol. Fr.*, 7 *Ser.*, **XVIII**, 1377–1385.

Bouchez, J. L. & Pecher, A. 1981. The Himalayan main central thrust and its quartz-rich tectonites in Central Nepal. *Tectonophysics* **78**, 23–50.

Brun, J. P. & Pons, J. 1981. Strain patterns of pluton emplacement in a crust undergoing non-coaxial deformation: Sierra Morena, Southern Spain. *J. Struct. Geol.* **3**, 219–229.

Courrioux, G. 1982. Exemple de mise en place d'un leucogranite pendant le fonctionnement d'une zone de cisaillement: le granite hercynien de Puentedeume (Galice, Espagne). *Bull. Soc. géol. Fr.*, 7 *Ser.*, **XXV**, 301–307.

Coward, M. P. 1981. Diapirism and gravity tectonics: report of a Tectonic Studies Group Conference held at Leeds University, 25–26 March 1980. *J. Struct. Geol.* **3**, 89–95.

Dixon, J. M. 1975. Finite strain and progressive deformation in models of diapiric structures. *Tectonophysics* **28**, 89–124.

Dunnet, D. 1969. A technique of finite strain analysis using elliptical particles. *Tectonophysics* **73**, 117–136.

Dunnet, D. & Siddans, A. W. B. 1971. Non-random sedimentary fabrics and their modification by strain. *Tectonophysics* **12**, 307–325.

Etchecopar, A. 1977. A plane kinematic model of progressive deformation in a polycrystalline aggregate. *Tectonophysics* **39**, 121–139.

Gapais, D. 1979. Déformation progressive d'un quartzite dans une zone plissée (segment hercynien de Bretagne Centrale). *Bull. Minéral.* **102**, 249–264.

Gagny, Cl., Courrioux, G., Cuenin, O., Jacquot, T. & Leistel, J. M.

1984. Contrôle structural de la métallogenèse dans la région d'Echassières par une zone de cisaillement regionale orientée a N 60 E (Massif Central Francais). *C.r. hebd. Séanc. Acad. Sci., Paris* **298**, serie II, 459–462.

Guillet, Ph., Bouchez, J. L. & Vigneresse, J. L. 1985. Le complexe granitique de Plouaret (Bretagne): mise en évidence structurale et gravimétrique de diapirs emboités. *Bull. Soc. géol. Fr.*, 8 *Ser.*, **I**, 503–513.

Halliday, A. N., Stephens, W. E. & Harmon, R. S. 1980. Rb–Sr and O isotopic relationships in three zoned Caledonian granitic plutons, Southern Uplands, Scotland: evidence for varied sources and hybridization of magmas. *J. geol. Soc. Lond.* **137**, 329–348.

Halliday, A. N. 1983. Crustal melting and the genesis of isotopically and chemically zoned plutons in the Southern Uplands of Scotland. In: *Migmatites, Melting and Metamorphism* (edited by Atherton, M. P. & Gribble, C. D.). Shiva geology series, Orpington, 54–61.

Holder, M. T. 1979. An emplacement mechanism for post-tectonic granites and its implications for the geochemical features. In: *Origin of Granite Batholiths, Geochemical Evidence* (edited by Atherton, M. P. & Tarney, J.). Shiva geology series, Orpington, 116–128.

Holder, M. T. 1983. Discussion on convection and crystallization in the Criffel Dalbeattie pluton. *J. geol. Soc. Lond.* **40**, 311–313.

Hutton, D. H. W. 1982a. A tectonic model for the emplacement of the main Donegal granite, N.W. Ireland. *J. geol. Soc. Lond.* **39**, 615–631.

Hutton, D. H. W. 1982b. A method for the determination of the initial shapes of deformed xenoliths in granitoids. *Tectonophysics* **85**, 45–50.

Kafafy, A. M. & Tarling, D. H. 1985. Magnetic fabric in some granitic aureoles, Southern Uplands. *J. Soc. geol. Lond.* **142**, 1007–1014.

Kemp, A. E. S., Oliver, G. H. J. & Baldwin, J. R. 1985. Low-grade metamorphism and accretion tectonics: Southern Uplands Terrain, Scotland. *Mineralog. Mag.* **49**, 335–344.

Lagarde, J. L. & Choukroune, P. 1982. Cisaillement ductile et granitoïdes syntectoniques: l'exemple du massif hercynien des Jebilets. *Bull. Soc. géol. Fr.*, 7 *Ser.*, **XXIV**, 299–307.

Law, R. D., Knipe, R. J. & Dayan, H. 1984. Strain path partitioning within thrust sheets: microstructural and petrofabric evidence from the Moine Thrust Zone at Loch Eriboll, northwest Scotland. *J. Struct. Geol.* **6**, 477–498.

Leggett, J. K., McKerrow, W. S. & Soper, N. J. 1983. A model for the crustal evolution of Southern Scotland. *Tectonics* **2**, 187–210.

Lister, G. S. & Hobbs, B. E. 1980. The simulation of fabric development during plastic deformation and its applications to quartzite. The influence of deformation history. *J. Struct. Geol.* **2**, 355–370.

Lister, G. S. & Williams, P. F. 1979. Fabric development in shear zones: Theoretical controls and observed phenomena. *J. Struct. Geol.* **1**, 283–297.

McKerrow, W. S., Leggett, J. K. & Eales, M. H. 1977. Imbricate thrust model of the Southern Uplands of Scotland. *Nature* **267**, 237–239.

Morgan, J. 1980. Deformation due to the distension of cylindrical igneous contacts: a kinematic model. *Tectonophysics* **66**, 167–178.

Murphy, F. C. & Hutton, D. H. W. 1986. Is the Southern Uplands of Scotland really an accretionary prism? *Geology* **14**, 354–357.

Oliver, G. H. J., Smellie, J. L., Thomas, L. J., Casey, D. M., Kemp, A. E. S., Evans, L. J., Baldwin, J. R. & Hepworth, B. C. 1984. Early Palaeozoic metamorphic history of the Midland Valley, Southern Uplands, Longford Down massif and the Lake District, British Isles. *Trans. R. Soc. Edinb.: Earth Sciences* **75**, 245–258.

Phillips, W. J. 1956. The Criffel Dalbeattie granodiorite complex. *Qt. J. geol. Soc. Lond.* **138**, 351–366.

Phillips, W. J., Fuge, R. &. Phillips, N. 1981. Convection and crystallization in the Criffel Dalbeattie pluton. *J. geol. Soc. Lond.* **138**, 351–366.

Phillips, W. J., Fuge, R. &. Phillips, N. 1983. Discussion on convection and crystallization in the Criffel Dalbeattie pluton. Reply. *J. geol. Soc. Lond.* **40**, 311–313.

Pitcher, W. S. 1979. The nature, ascent and emplacement of granite magmas. *J. geol. Soc. Lond.* **136**, 627–662.

Ramberg, H. 1967. *Gravity, Deformation and the Earth's Crust as Studied by Centrifuged Models.* Academic Press, London.

Ramberg, H. 1970. Model studies in relation to intrusion of plutonic bodies (edited by Newall, G. & Rast, N.). *Geol. J. Special Issue* **2**, 261–285.

Ramsay, J. G. 1975. The structure of the Chindamora Batholith. *19th Ann. Rept. Res. Inst. Afr. Geol.*, Univ. Leeds, 81.

Ramsay, J. G. 1981. Emplacement mechanics of the Chindamora Batholith, Zimbabwe. In: M. P. Coward: Diapirism and gravity tectonics: report of a Tectonic Studies Group conference held at Leeds University, 25–26 March 1980. *J. Struct. Geol.* **3**, 93.

Sampson, R. 1975. The surface II graphics system. In: *Display and Analysis of Spatial Data* (edited by Davis, J. C. & McCullagh, M. J.). John Wiley, London 244–266.

Schmid, S. M., Casey, M. & Starkey, J. 1981. An illustration of the advantages of a complete texture analysis described by the orientation distribution function (O.D.F) using quartz pole figure data. *Tectonophysics* **78**, 101–107.

Schwerdtner, W. M. & Troeng, B. 1978. Strain distribution within arcuate diapiric ridges of silicone putty. *Tectonophysics* **50**, 13–28.

Schwerdtner, W. M. 1981. Identification of gneiss diapirs. In: M. P. Coward: Diapirism and gravity tectonics: report of a Tectonic Studies Group conference held at Leeds University, 25–26 March 1980. *J. Struct. Geol.* **3**, 90.

Simpson, C. & Schmid, S. 1983. An evaluation of criteria to deduce the sence of movement in sheared rocks. *Bull. geol. Soc. Am.* **94**, 1281–1288.

Soper, N. J. & Hutton, D. H. W. 1984. Late Caledonian sinistral displacements in Britain: implications for a three plate collision model. *Tectonics* **3**, 781–794.

Stephens, W. E. & Halliday, A. N. 1980. Discontinuities in the composition of a zoned pluton, Criffel, Scotland. *Bull. geol. Soc. Am.* **91**, 165–170.

Stephens, W. E., Whitley, J. E., Thirwall, M. F. & Halliday, A. N. 1985. The Criffel zoned pluton: correlated behaviour of rare earth elements abundances with isotopic systems. *Contr. Miner. Petrol.* **89**, 226–238.

Talbot, C. J. 1977. Inclined asymmetric upward-moving gravity structures. *Tectonophysics* **42**, 159–181.

Thornton, C. P. & Tuttle, O. F. 1960. Chemistry of igneous rocks, differentiation index. *Am. J. Sci.* **258**, 664–684.

Tullis, J. A., Christie, J. M. & Griggs, D. T. 1973. Microstructures of experimentally deformed quartzites. *Bull. geol. Soc. Am.* **84**, 297–314.